

Probing Earth's Upper Mantle With Daily Magnetic Field Variations. Exploring a Physics-Based Parametrization of the Source

Géraldine Zenhäuser (✉ geraldine.zenhaeuser@erdw.ethz.ch)

ETH Zürich: Eidgenössische Technische Hochschule Zurich <https://orcid.org/0000-0001-9401-4910>

Alexey Kuvshinov

ETH Zürich: Eidgenössische Technische Hochschule Zurich

Martina Guzavina

ETH Zürich: Eidgenössische Technische Hochschule Zurich

Astrid Maute

NCAR: National Center for Atmospheric Research

Full paper

Keywords: Electromagnetic induction, Ionospheric current systems, Magnetic field variations, Principal component analysis

Posted Date: February 24th, 2021

DOI: <https://doi.org/10.21203/rs.3.rs-230799/v1>

License:  This work is licensed under a Creative Commons Attribution 4.0 International License.

[Read Full License](#)

Abstract

The electromagnetic (EM) field variations capable of probing the electrical conductivity of the upper mantle and mantle transition zone have a period range between a few hours and one day. At these periods, the dominant source of the EM signals is the ionospheric current system, which has a complex spatial and temporal structure. A concept of global-to-local (G2L) transfer functions can handle spatially complex source by relating global source expansion coefficients with locally measured magnetic (or/and electric) fields. When estimating the G2L transfer functions, the source is commonly expanded into spherical harmonics (SH). In this paper, we explore an alternative parametrization of the source based on a principal component analysis (PCA) of the Fourier transformed output from the physics-based Thermosphere Ionosphere Electrodynamics General Circulation Model (TIE-GCM). Specifically, we investigate whether magnetic fields computed in the realistic three-dimensional conductivity model of Earth excited by the PCA-based source agree better with observatory data than those computed in the same model but induced by the SH-based source. Using PCA to capture the source current compared to SH parametrization, we found that agreement with the observatory data is better during magnetically disturbed times and at shorter periods. Vice versa, it is poorer during magnetically quiet times and at longer periods.

Full Text

Due to technical limitations, full-text HTML conversion of this manuscript could not be completed. However, the latest manuscript can be downloaded and [accessed as a PDF](#).

Figures

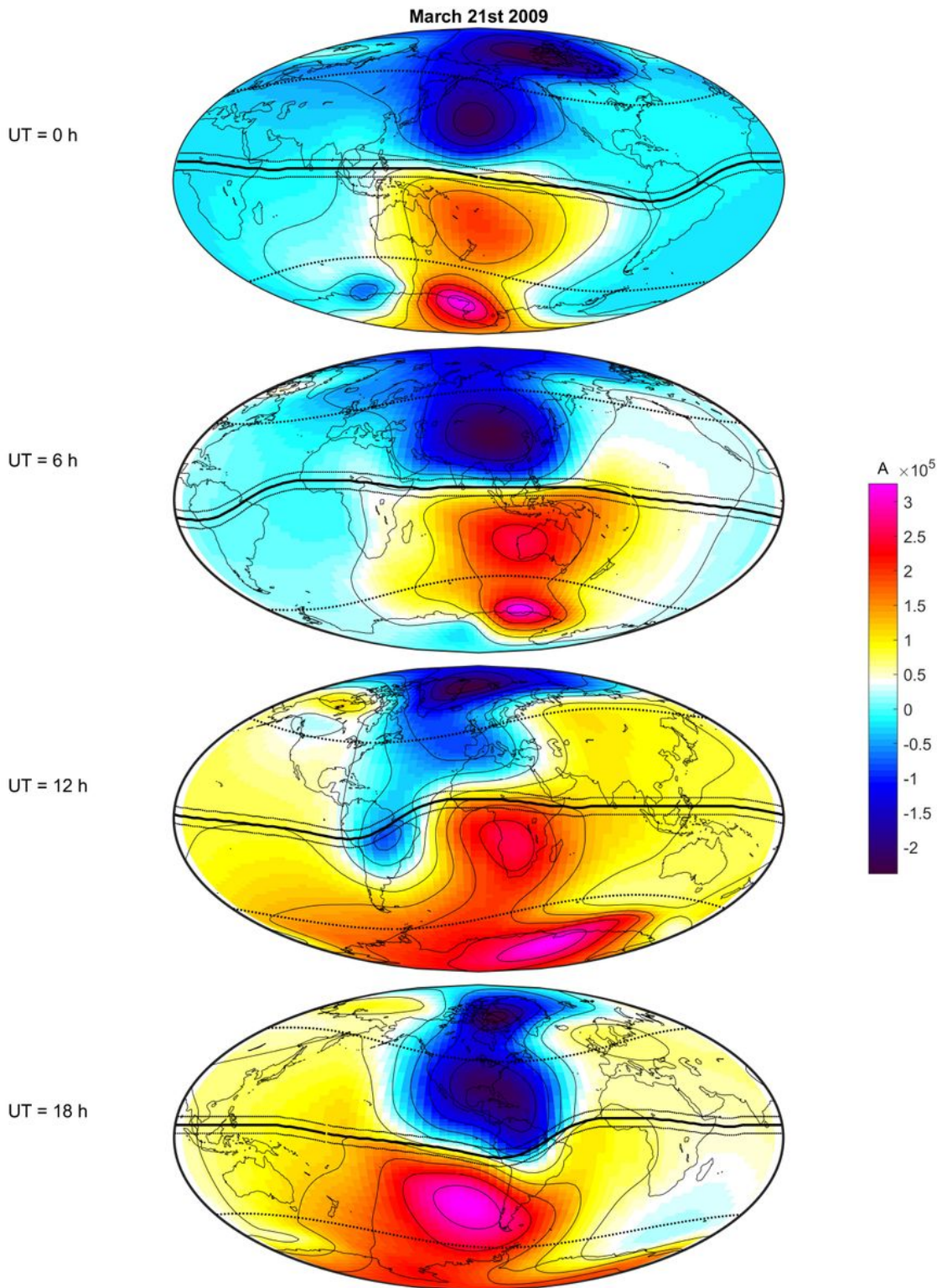


Figure 1

TIE-GCM stream function. The authors acknowledge British Geological Survey, World Data Center Geomagnetism (Edinburgh), INTERMAGNET, and the many institutes worldwide that operate magnetic observatories. MG was supported by ETH Grant No. ETH-3215-2. GZ and AK were partly supported in the framework of Swarm DISC activities, funded by ESA contact no. 4000109587, with support from EO Science for Society.

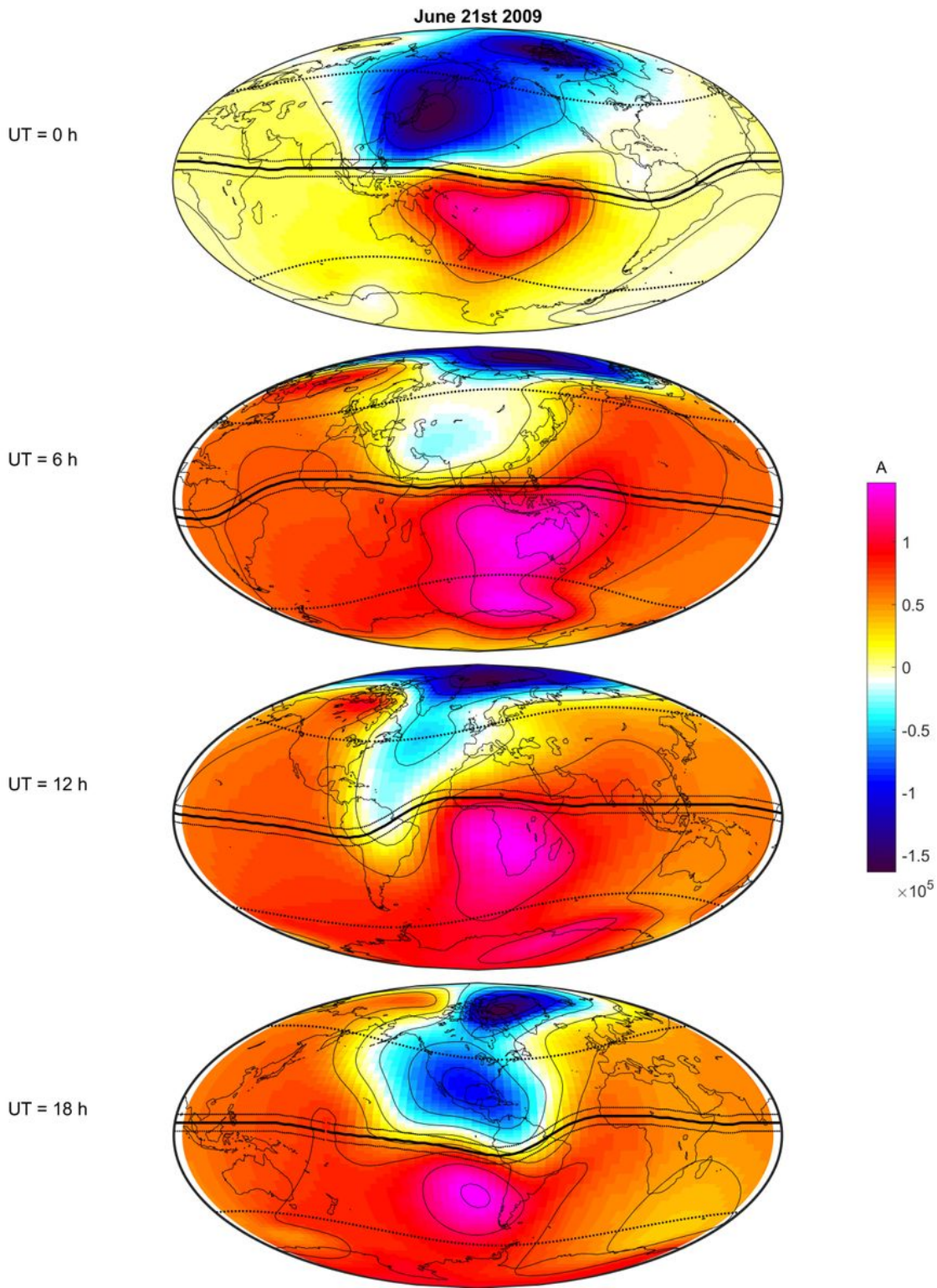


Figure 2

TIE-GCM stream function output. Time snapshots of TIE-GCM stream function $\Psi(t)$ on June 21 2009 (solstice).

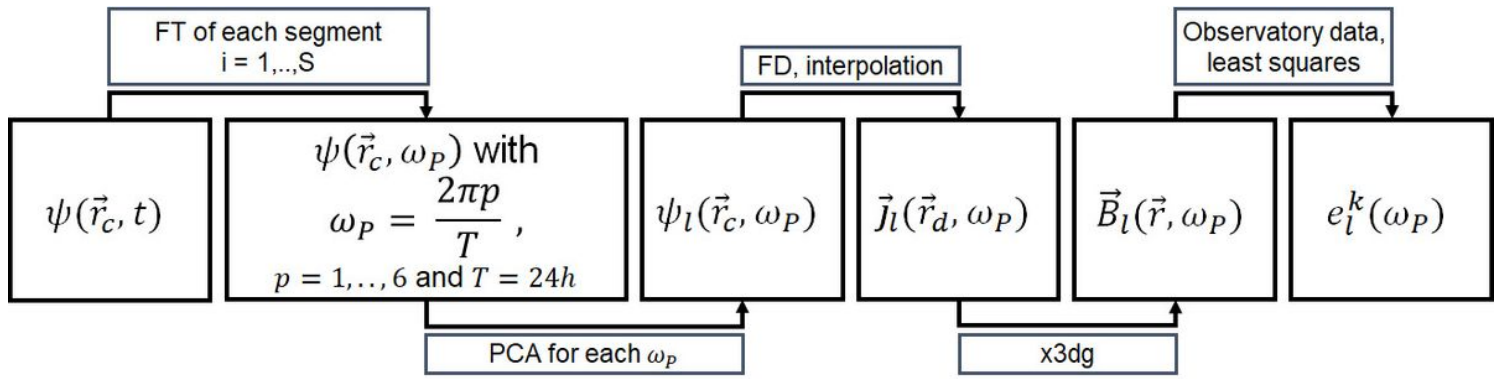


Figure 3

Workflow. Workflow used to process the data. FD stands for finite differences. $\sim rc$ and $\sim rd$ denote a "coarse" and "dense" grid, respectively. See details in the text.

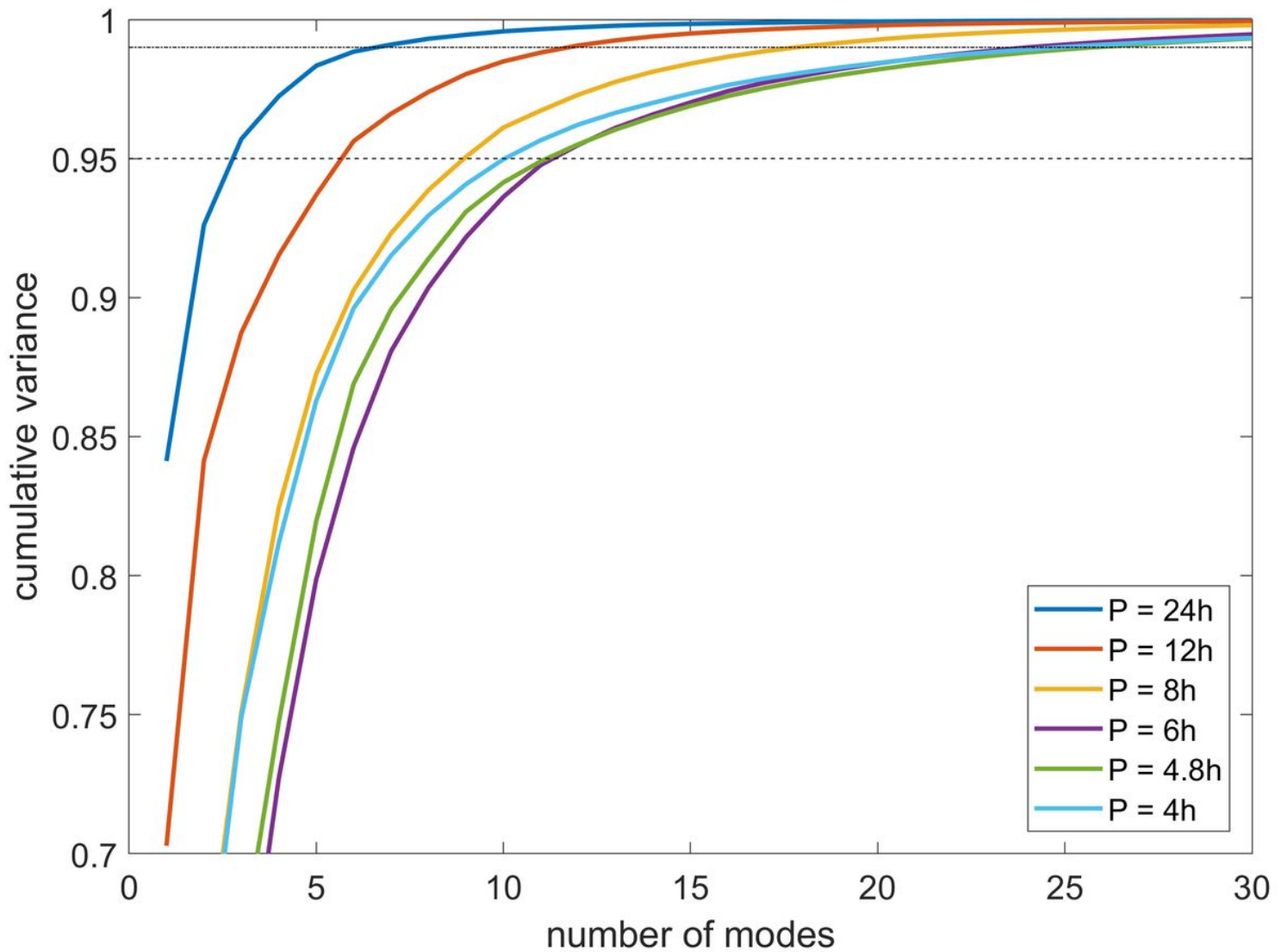


Figure 4

Cumulative variance. Cumulative variance for the rst 30 spatial modes of PCA applied to the whole 338 days TIE-GCM time series and plotted for each period, $P = 24, 12, 8, 6, 4.8,$ and 4 hours. FT segment length is 24 hours. Dashed and dash-dotted lines mark the 95% and 99% thresholds, respectively.

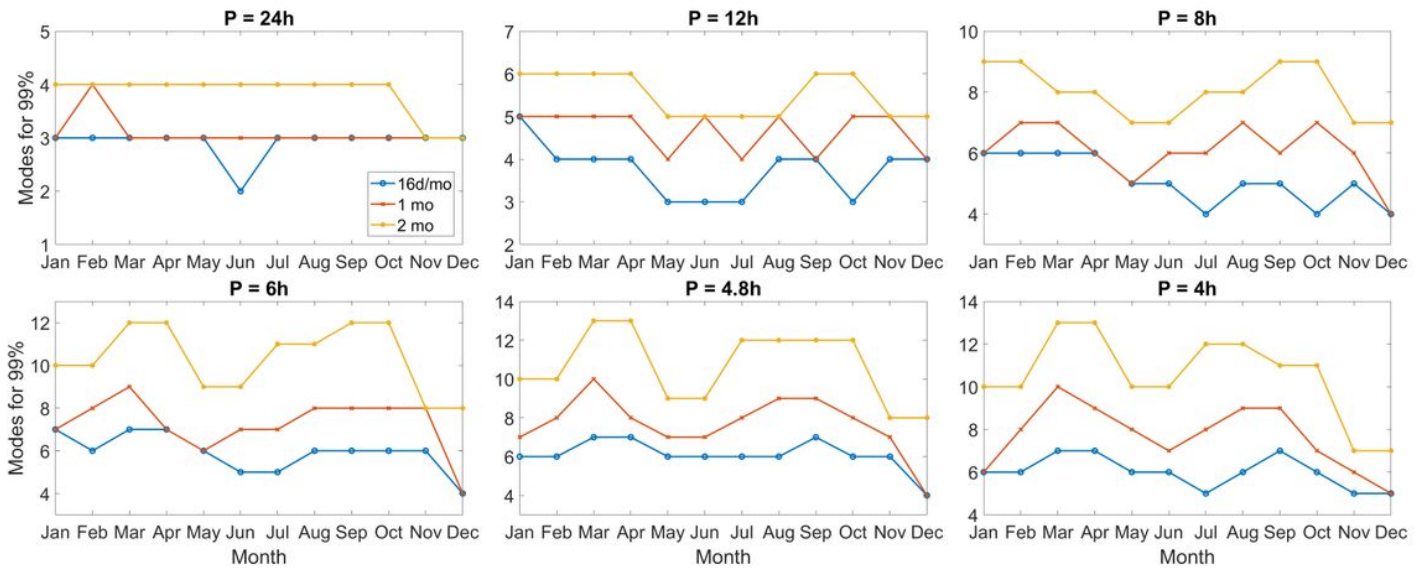


Figure 5

Time series variations. Number of modes needed to explain 99% variance for each period, $P = 24, 12, 8, 6, 4.8,$ and 4 hours. The time series length is 16 days, 1 month, and 2 months (adjacent months, thus January-February, March-April, May-June, etc.). The FT segment length for all PCA runs is 24 hours. Note that January and December do not have the full months of data available, as the TIE-GCM stream function spans 13.01.2009-16.12.2009.

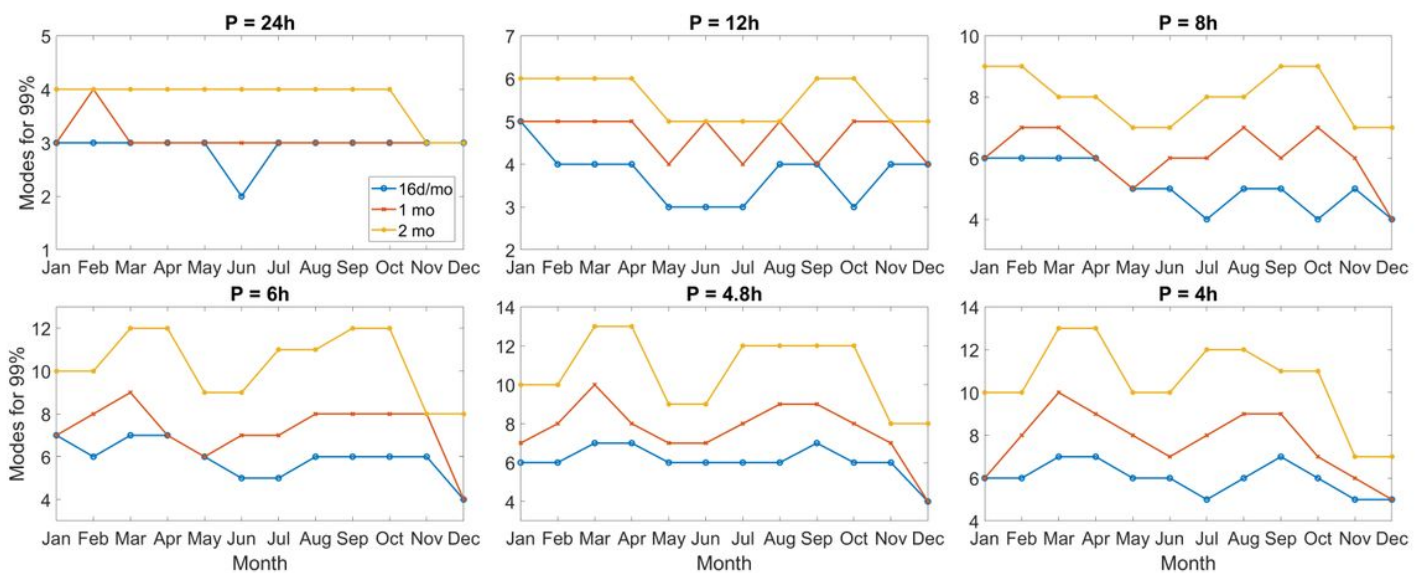


Figure 6

FT segment variations. Number of modes needed to explain 99% variance for each period, $P = 24, 12, 8, 6, 4.8,$ and 4 hours. The time series length is restricted to single months, and the FT segment length is varied between 24, 48, and 72 hours. Note that January and December do not have the full months of data available, as the stream function spans 13.01.2009-16.12.2009.

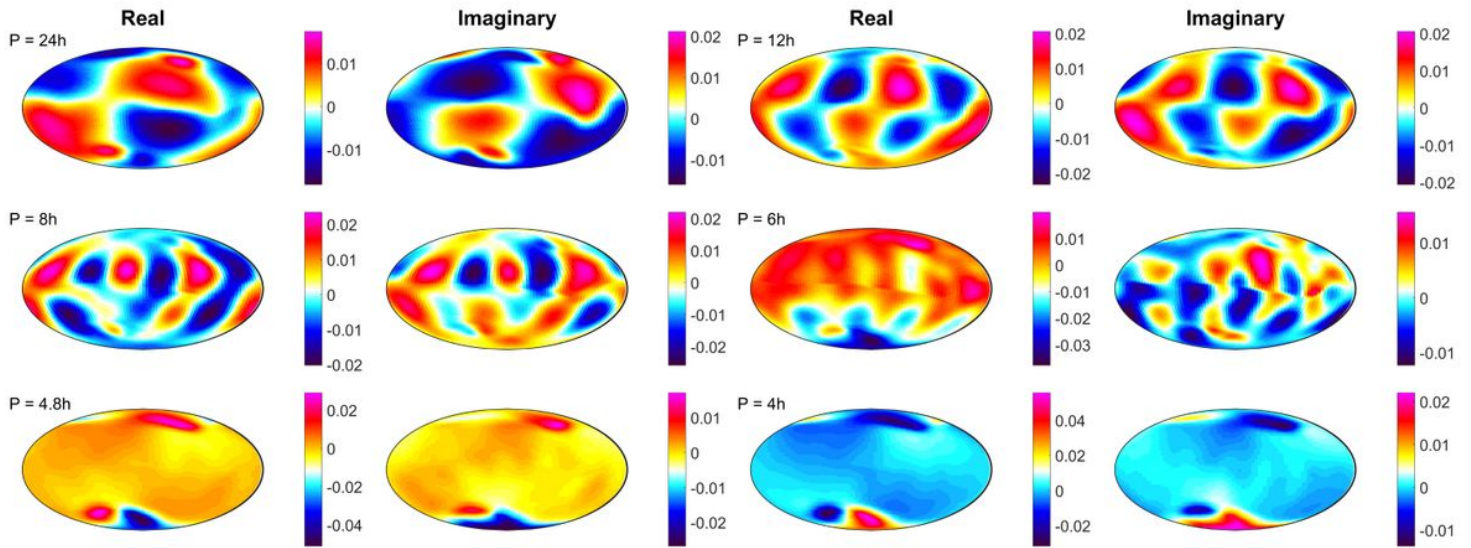


Figure 7

Spatial modes. Maps of the rst, dominant mode for each period $P = 24, 12, 8, 6, 4.8,$ and 4 hours for PCA for the whole time series with an FT segment length of 24 hours. Both real and imaginary parts are displayed. Scaling is normalized and unit-less.

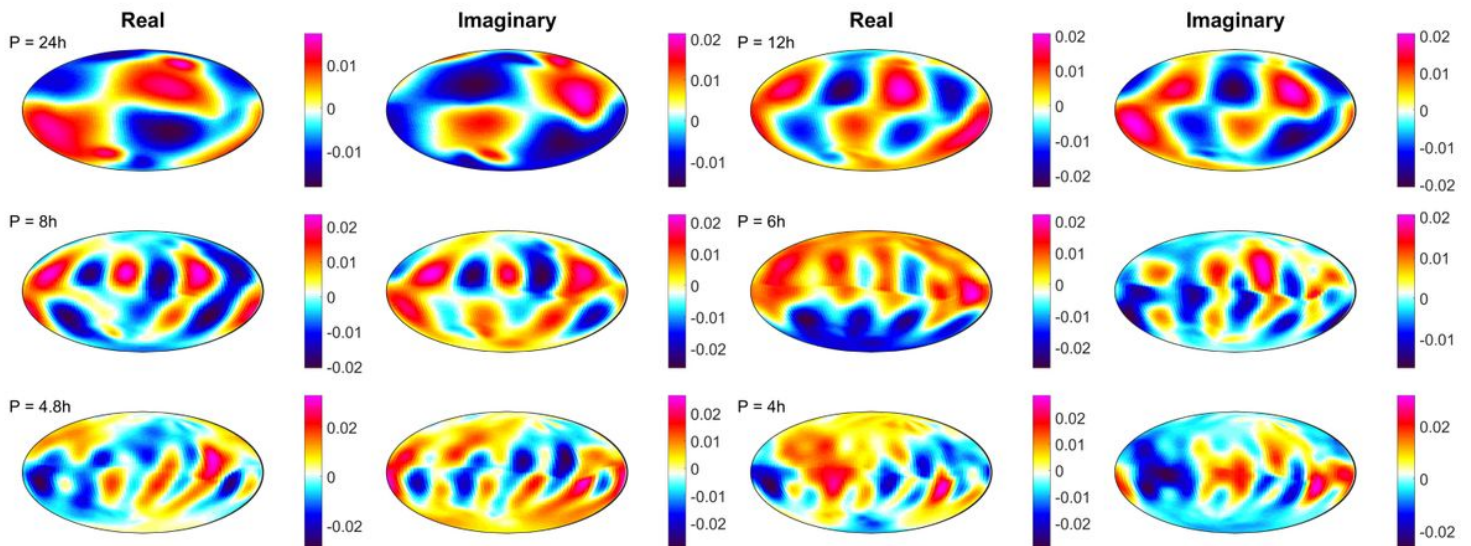


Figure 8

Spatial modes for 72h FT segments. Maps of the rst, dominant mode for each period $P = 24, 12, 8, 6, 4.8,$ and 4 hours for PCA for the whole time series with an FT segment length of 72 hours. Both real and imaginary parts are displayed. Scaling is normalized and unit-less.

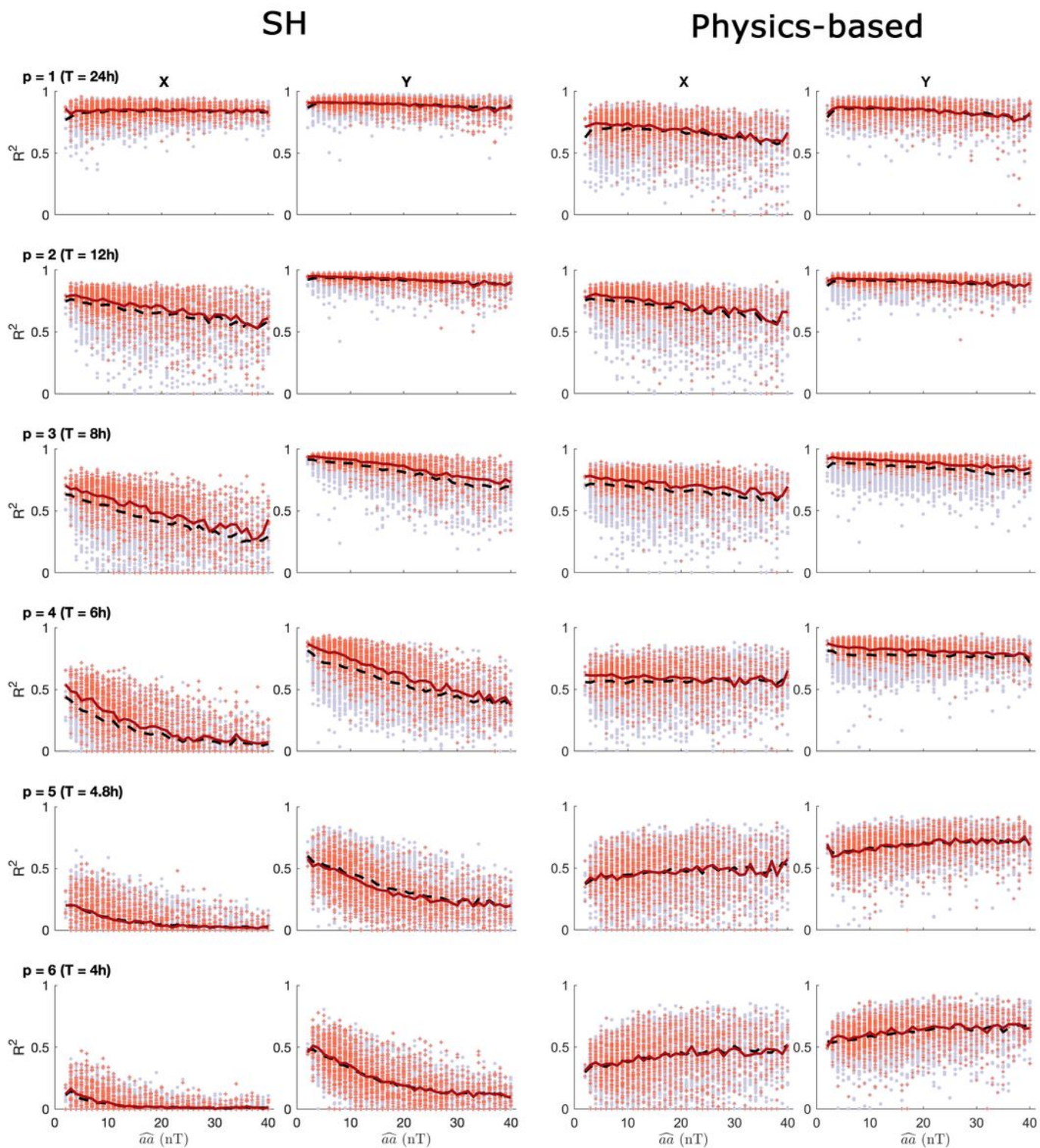


Figure 9

R^2 results for X and Y components. Coefficient of determination R^2 for periods $P = 24, 12, 8, 6, 4.8,$ and 4 hours for magnetic field components X and Y. $X = -B\theta$ and $Y = B\phi$ denote the north and east components, respectively. Stations for estimating the Sq coefficients are limited to mid-latitudes between $\pm 5^\circ$ and 55° . Two leftmost columns: R^2 computed by Guzavina et al (2019) using a spherical harmonic parameterization of the source. Two rightmost columns: R^2 computed using a PCA-based

parameterization of the source. The number of modes corresponds to the 99% threshold for the variance of the TIE-GCM stream function. PCA was applied to the whole 338 days TIE-GCM time series. FT segment length was taken as 24 hours. Grey circles mark all days, and red pluses mark equinoctial days. The lines mark their mean values, respectively. The aa index indicates the level of geomagnetic disturbance, where a larger index stands for a more disturbed day; more details about this index can be found in (Guzavina et al, 2019).

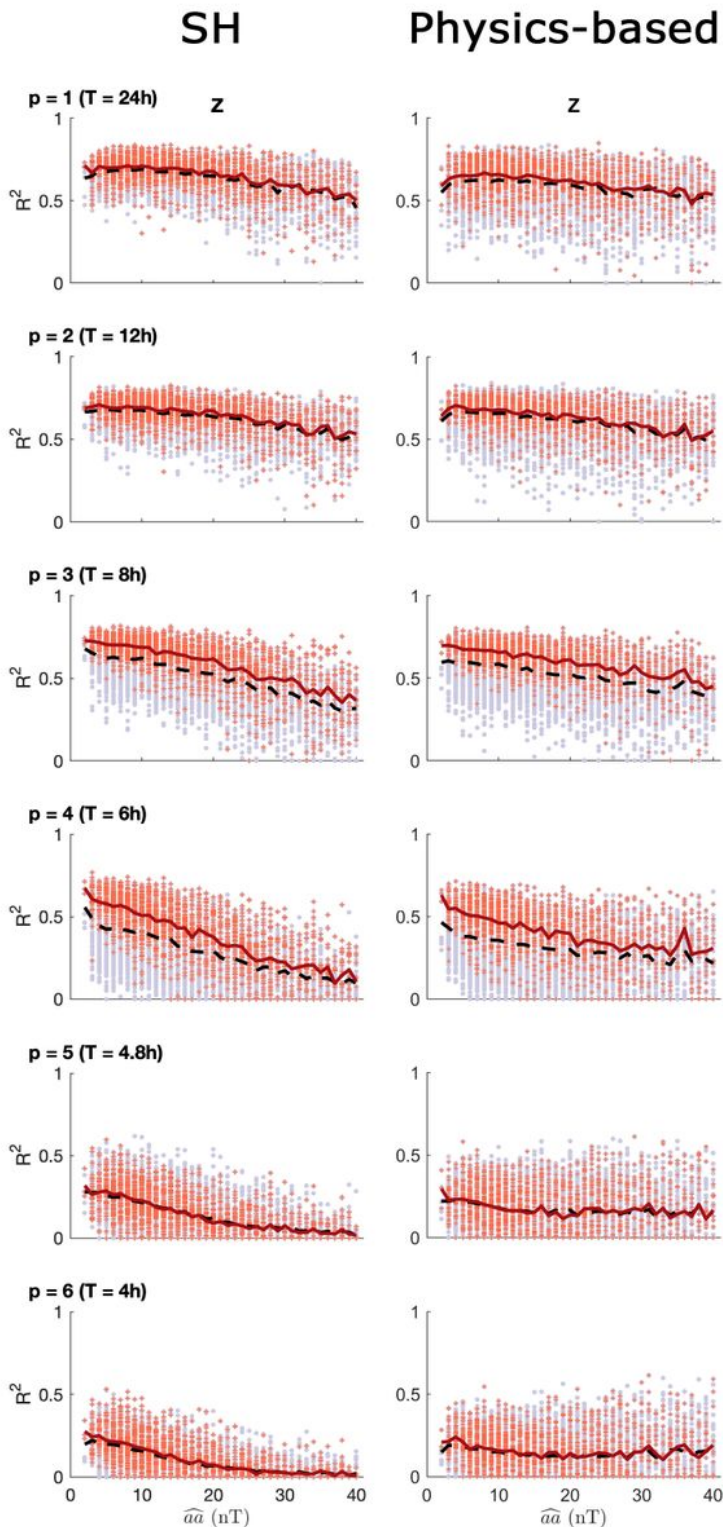


Figure 10

R2 results for Z component. Same as in Figure 9 but for Z component.

Supplementary Files

This is a list of supplementary files associated with this preprint. Click to download.

- [graphicalabstract.png](#)